Employment of triketone to construct dysprosium(III) single-molecule magnet

Chao Wang,[a] Shuang-Yan Lin,[a] Jianfeng Wu,[a,b] Sen-Wen Yuan[a] and Jinkui Tang*[a]

[a] *State Key Laboratory of Rare Earth Resource Utilization, Changchun Institute of Applied Chemistry, Chinese Academy of Sciences, Changchun 130022, P. R. China*
[b] *University of Chinese Academy of Sciences, Beijing, 100049, P. R. China*

Table S1. Selected bond lengths (Å) and angles (º) for complex **1**

Dy(1)-O(3)	2.245(12)	Dy(1)-O(6)	2.253(11)
Dy(1)-O(9)	2.306(13)	Dy(1)-O(8)	2.349(11)
Dy(1)-O(5)	2.406(10)	Dy(1)-O(2)	2.441(11)
Dy(1)-N(2)	2.558(14)	Dy(1)-N(1)	2.562(14)
Dy(2)-O(1)	2.229(12)	Dy(2)-O(4)	2.271(12)
Dy(2)-O(7)	2.313(13)	Dy(2)-O(8)	2.390(10)
Dy(2)-O(2)	2.415(11)	Dy(2)-O(5)	2.452(10)
Dy(2)-N(3)	2.501(15)	Dy(2)-N(4)	2.528(14)
O(3)-Dy(1)-O(6)	84.3(4)	O(3)-Dy(1)-O(9)	144.5(4)
O(6)-Dy(1)-O(9)	77.7(5)	O(3)-Dy(1)-O(8)	140.2(4)
O(6)-Dy(1)-O(8)	131.1(4)	O(9)-Dy(1)-O(8)	71.2(4)
O(3)-Dy(1)-O(5)	114.5(4)	O(6)-Dy(1)-O(5)	73.9(4)
O(9)-Dy(1)-O(5)	89.7(4)	O(8)-Dy(1)-O(5)	69.2(3)
O(3)-Dy(1)-O(2)	74.9(4)	O(6)-Dy(1)-O(2)	122.2(4)
O(9)-Dy(1)-O(2)	140.4(4)	O(8)-Dy(1)-O(2)	70.5(4)
O(5)-Dy(1)-O(2)	67.6(4)	O(3)-Dy(1)-N(2)	73.3(4)
O(6)-Dy(1)-N(2)	84.6(4)	O(9)-Dy(1)-N(2)	74.7(5)
O(8)-Dy(1)-N(2)	120.6(4)	O(5)-Dy(1)-N(2)	155.8(4)
O(2)-Dy(1)-N(2)	135.4(4)	O(3)-Dy(1)-N(1)	80.4(4)
O(6)-Dy(1)-N(1)	148.3(4)	O(9)-Dy(1)-N(1)	99.4(5)
O(8)-Dy(1)-N(1)	74.9(4)	O(5)-Dy(1)-N(1)	137.7(4)
O(2)-Dy(1)-N(1)	80.1(4)	N(2)-Dy(1)-N(1)	64.5(4)
O(1)-Dy(2)-O(4)	79.1(4)	O(1)-Dy(2)-O(7)	86.9(5)
O(4)-Dy(2)-O(7)	148.5(4)	O(1)-Dy(2)-O(8)	136.8(4)
O(4)-Dy(2)-O(8)	136.6(4)	O(7)-Dy(2)-O(8)	70.8(4)
O(1)-Dy(2)-O(2)	75.9(4)	O(4)-Dy(2)-O(2)	108.0(4)
O(7)-Dy(2)-O(2)	95.6(4)	O(8)-Dy(2)-O(2)	70.2(4)
O(1)-Dy(2)-O(5)	121.8(4)	O(4)-Dy(2)-O(5)	71.8(4)
O(7)-Dy(2)-O(5)	138.4(4)	O(8)-Dy(2)-O(5)	67.8(3)
O(2)-Dy(2)-O(5)	67.2(4)	O(1)-Dy(2)-N(3)	142.8(5)
O(4)-Dy(2)-N(3)	82.7(4)	O(7)-Dy(2)-N(3)	92.1(4)

O(8)-Dy(2)-N(3)	76.4(4)	O(2)-Dy(2)-N(3)	140.9(4)
O(5)-Dy(2)-N(3)	81.8(4)	O(1)-Dy(2)-N(4)	78.4(5)
O(4)-Dy(2)-N(4)	72.9(4)	O(7)-Dy(2)-N(4)	76.7(4)
O(8)-Dy(2)-N(4)	128.1(4)	O(2)-Dy(2)-N(4)	153.5(4)
O(5)-Dy(2)-N(4)	134.1(4)	N(3)-Dy(2)-N(4)	65.4(5)
Dy(1)-O(2)-Dy(2)	97.5(4)	Dy(1)-O(5)-Dy(2)	97.4(3)
Dy(1)-O(8)-Dy(2)	100.7(4)		

Table S2. Selected bond lengths (Å) and angles (º) for complex **2**

N(1)-Nd(1)	2.610(3)	N(2)-Nd(1)	2.637(4)
N(3)-Nd(2)	2.642(4)	N(4)-Nd(2)	2.586(4)
Nd(1)-O(4)	2.294(3)	Nd(1)-O(1)	2.342(3)
Nd(1)-O(8)	2.371(3)	Nd(1)-O(7)	2.423(3)
Nd(1)-O(5)	2.496(3)	Nd(1)-O(2)	2.548(3)
Nd(2)-O(3)	2.300(3)	Nd(2)-O(6)	2.339(3)
Nd(2)-O(8)	2.376(3)	Nd(2)-O(9)	2.419(3)
Nd(2)-O(2)	2.505(3)	Nd(2)-O(5)	2.560(3)
O(4)-Nd(1)-O(1)	84.60(11)	O(4)-Nd(1)-O(8)	137.29(10)
O(1)-Nd(1)-O(8)	132.98(11)	O(4)-Nd(1)-O(7)	82.64(12)
O(1)-Nd(1)-O(7)	154.99(10)	O(8)-Nd(1)-O(7)	68.32(11)
O(4)-Nd(1)-O(5)	74.81(10)	O(1)-Nd(1)-O(5)	116.24(10)
O(8)-Nd(1)-O(5)	70.33(9)	O(7)-Nd(1)-O(5)	80.87(10)
O(4)-Nd(1)-O(2)	117.54(11)	O(1)-Nd(1)-O(2)	71.91(10)
O(8)-Nd(1)-O(2)	69.35(10)	O(7)-Nd(1)-O(2)	133.10(9)
O(5)-Nd(1)-O(2)	66.59(9)	O(4)-Nd(1)-N(1)	85.95(11)
O(1)-Nd(1)-N(1)	85.66(11)	O(8)-Nd(1)-N(1)	112.24(10)
O(7)-Nd(1)-N(1)	72.08(11)	O(5)-Nd(1)-N(1)	148.58(11)
O(2)-Nd(1)-N(1)	144.72(10)	O(4)-Nd(1)-N(2)	141.66(11)
O(1)-Nd(1)-N(2)	72.77(11)	O(8)-Nd(1)-N(2)	78.11(10)
O(7)-Nd(1)-N(2)	105.22(11)	O(5)-Nd(1)-N(2)	143.00(10)
O(2)-Nd(1)-N(2)	84.75(10)	N(1)-Nd(1)-N(2)	62.33(12)
O(3)-Nd(2)-O(6)	88.98(11)	O(3)-Nd(2)-O(8)	135.37(10)
O(6)-Nd(2)-O(8)	131.48(11)	O(3)-Nd(2)-O(9)	81.53(12)
O(6)-Nd(2)-O(9)	154.10(11)	O(8)-Nd(2)-O(9)	68.08(11)
O(3)-Nd(2)-O(2)	74.57(10)	O(6)-Nd(2)-O(2)	117.80(10)
O(8)-Nd(2)-O(2)	70.04(9)	O(9)-Nd(2)-O(2)	82.90(10)
O(3)-Nd(2)-O(5)	119.20(10)	O(6)-Nd(2)-O(5)	71.85(10)
O(8)-Nd(2)-O(5)	69.14(9)	O(9)-Nd(2)-O(5)	133.61(10)
O(2)-Nd(2)-O(5)	66.28(9)	O(3)-Nd(2)-N(4)	82.32(12)
O(6)-Nd(2)-N(4)	82.77(11)	O(8)-Nd(2)-N(4)	115.98(11)

O(9)-Nd(2)-N(4)	72.15(12)	O(2)-Nd(2)-N(4)	148.16(12)
O(5)-Nd(2)-N(4)	145.51(12)	O(3)-Nd(2)-N(3)	141.99(11)
O(6)-Nd(2)-N(3)	73.76(11)	O(8)-Nd(2)-N(3)	76.98(10)
O(9)-Nd(2)-N(3)	99.30(12)	O(2)-Nd(2)-N(3)	143.44(10)
O(5)-Nd(2)-N(3)	87.78(11)	N(3)-Nd(2)-N(4)	62.41(13)
Nd(1)-O(2)-Nd(2)	95.71(10)	Nd(1)-O(5)-Nd(2)	95.64(9)
Nd(1)-O(8)-Nd(2)	104.22(10)		

Table S3. Selected bond lengths (Å) and angles (º) for complex **10**

Yb(2)-N(1)	2.502(4)	Yb(2)-N(2)	2.474(3)
Yb(1)-N(3)	2.528(4)	Yb(1)-N(4)	2.503(3)
Yb(1)-O(1)	2.222(3)	Yb(1)-O(2)	2.377(3)
Yb(2)-O(2)	2.407(3)	Yb(2)-O(3)	2.216(3)
Yb(2)-O(4)	2.199(3)	Yb(2)-O(5)	2.370(3)
Yb(1)-O(5)	2.423(3)	Yb(1)-O(6)	2.213(3)
Yb(2)-O(7)	2.278(3)	Yb(1)-O(8)	2.313(3)
Yb(2)-O(8)	2.350(3)	Yb(1)-O(9)	2.260(3)
O(6)-Yb(1)-O(1)	83.25(11)	O(6)-Yb(1)-O(9)	143.56(10)
O(1)-Yb(1)-O(9)	76.75(12)	O(6)-Yb(1)-O(8)	139.96(10)
O(1)-Yb(1)-O(8)	132.52(10)	O(9)-Yb(1)-O(8)	72.78(10)
O(6)-Yb(1)-O(2)	114.02(10)	O(1)-Yb(1)-O(2)	75.66(10)
O(9)-Yb(1)-O(2)	90.26(11)	O(8)-Yb(1)-O(2)	69.04(10)
O(6)-Yb(1)-O(5)	75.24(10)	O(1)-Yb(1)-O(5)	122.96(11)
O(9)-Yb(1)-O(5)	141.11(10)	O(8)-Yb(1)-O(5)	69.82(9)
O(2)-Yb(1)-O(5)	66.80(9)	O(6)-Yb(1)-N(4)	73.02(11)
O(1)-Yb(1)-N(4)	82.28(12)	O(9)-Yb(1)-N(4)	74.33(12)
O(8)-Yb(1)-N(4)	121.81(11)	O(2)-Yb(1)-N(4)	155.55(11)
O(5)-Yb(1)-N(4)	136.15(11)	O(6)-Yb(1)-N(3)	80.41(11)
O(1)-Yb(1)-N(3)	146.73(11)	O(9)-Yb(1)-N(3)	100.18(12)
O(8)-Yb(1)-N(3)	75.06(10)	O(2)-Yb(1)-N(3)	137.57(10)
O(5)-Yb(1)-N(3)	80.28(10)	N(4)-Yb(1)-N(3)	65.30(12)
O(4)-Yb(2)-O(3)	78.40(12)	O(4)-Yb(2)-O(7)	84.92(12)
O(3)-Yb(2)-O(7)	146.82(11)	O(4)-Yb(2)-O(8)	136.39(11)
O(3)-Yb(2)-O(8)	137.98(10)	O(7)-Yb(2)-O(8)	71.75(10)
O(4)-Yb(2)-O(5)	76.17(11)	O(3)-Yb(2)-O(5)	108.05(11)
O(7)-Yb(2)-O(5)	95.28(11)	O(8)-Yb(2)-O(5)	70.14(9)
O(4)-Yb(2)-O(2)	122.31(11)	O(3)-Yb(2)-O(2)	72.92(10)
O(7)-Yb(2)-O(2)	139.45(10)	O(8)-Yb(2)-O(2)	67.93(10)
O(2)-Yb(2)-O(5)	67.19(9)	O(4)-Yb(2)-N(2)	142.95(12)
O(3)-Yb(2)-N(2)	83.25(11)	O(7)-Yb(2)-N(2)	93.62(12)

O(8)-Yb(2)-N(2)	76.49(11)	O(5)-Yb(2)-N(2)	140.59(11)
O(2)-Yb(2)-N(2)	81.38(11)	O(4)-Yb(2)-N(1)	77.62(12)
O(3)-Yb(2)-N(1)	72.50(12)	O(7)-Yb(2)-N(1)	76.04(12)
O(8)-Yb(2)-N(1)	128.23(12)	O(5)-Yb(2)-N(1)	153.01(11)
O(2)-Yb(2)-N(1)	134.61(11)	N(2)-Yb(2)-N(1)	66.20(12)
Yb(1)-O(2)-Yb(2)	97.79(10)	Yb(1)-O(5)-Yb(2)	97.54(10)
Yb(1)-O(8)-Yb(2)	101.27(10)		

IR spectra data of complexes **2**-**10** (cm^{-1})**:**

Complex **2**: 1625(m), 1602(w), 1553(m), 1518(w), 1494(w), 1427(w), 1262(vs), 1184(vs), 1161(vw), 1146(vw), 1125(m), 1100(m), 998(vw), 983(s), 883(s), 864(w), 833(s), 820(vw), 775(w), 752(w), 722(m).

Complex **3**: 1614(s), 1549(m), 1529(w), 1494(m), 1425(m), 1388(vw), 1347(w), 1269(vs), 1185(vs), 1145(vw), 1114(vs), 982(s), 885(s), 864(w), 843(m), 820(s), 769(w), 775(w), 722(m).

Complex **4**: 1614(s), 1549(m), 1531(vw), 1494(s), 1425(m), 1388(w), 1347(w), 1291(vw), 1270(vs), 1185(vs), 1145(vw), 1115(vs), 983(s), 884(s), 864(w), 843(w), 820(m), 779(vw),769(w), 755(w), 722(m).

Complex **5**: 1615(s), 1549(m), 1533(w), 1495(m), 1425(m), 1389(w), 1347(w), 1268(vs), 1184(vs), 1145(vw), 1112(vs), 983(s), 885(s), 864(w), 843(w), 819(s), 779(vw), 769(w), 755(w), 722(m).

Complex **6**: 1614(s), 1550(m), 1535(w), 1495(m), 1425(m), 1388(w), 1347(w), 1269(vs), 1184(vs), 1145(vw), 1113(vs), 984(s), 886(s), 864(vw), 844(w), 819(s), 779(vw), 769(w), 756(w), 722(m), 706(vw).

Complex **7**: 1615(s), 1552(m), 1537(w), 1496(m), 1425(m), 1389(w), 1345(w), 1268(vs), 1184(vs), 1144(vw), 1114(vs), 1037(vw), 986(s), 887(s), 865(vw), 844(w), 819(s), 779(vw), 770(w), 756(w), 722(m), 705(vw).

Complex **8**: 1615(s), 1552(m), 1537(w), 1497(m), 1479(vw), 1425(m), 1389(w), 1347(w), 1268(vs), 1184(vs), 1144(vw), 1114(vs), 1038(vw), 986(s), 887(s), 865(vw), 844(w), 819(s), 779(vw), 770(w), 756(w), 723(m), 705(vw).

Complex **9**: 1626(vw), 1615(s), 1553(m), 1538(w), 1522(vw), 1497(m), 1425(m), 1389(w), 1347(w), 1267(vs), 1185(vs), 1116(vs), 1038(vw), 988(s), 889(s), 865(vw), 845(w), 819(s), 770(vw), 756(w), 723(m).

Complex **10**: 1629(w), 1608(w), 1556(m), 1537(w), 1522(vw), 1499(m), 1425(m), 1266(vs), 1185(vs), 1118(vs), 1038(vw), 990(s), 890(s), 866(w), 845(w), 829(vw), 818(m), 771(w), 755(w),
740(vw), 723(m).

Elemental analysis found (calc) % of complexes **2**-**10**:

Complex **2**: C: 38.71(38.80) H: 1.63(1.59) N: 4.04(4.02).

Complex **3**: C: 38.52(38.46) H: 1.57(1.58) N: 4.02(3.99).

Complex **4**: C: 38.44(38.37) H: 1.60(1.57) N: 3.92(3.98).

Complex **5**: C: 38.01(38.09) H: 1.52(1.56) N: 4.00(3.95).

Complex **6**: C: 38.03(38.00) H: 1.55(1.56) N: 3.91(3.94).

Complex **7**: C: 37.59(37.68) H: 1.52(1.55) N: 3.93(3.91).
Complex **8**: C: 37.61(37.56) H: 1.53(1.54) N: 3.85(3.89).
Complex **9**: C: 37.40(37.47) H: 1.54(1.54) N: 3.91(3.88).
Complex **10**: C: 37.19(37.26) H: 1.55(1.53) N: 3.88(3.86).

The calculation result by SHAPE software:

Dy1：

HBPY-8	3 D6h	Hexagonal bipyramid
CU-8	4 Oh	Cube
SAPR-8	5 D4d	Square antiprism
TDD-8	6 D2d	Triangular dodecahedron
JGBF-8	7 D2d	Johnson gyrobifastigium J26
JETBPY-8	8 D3h	Johnson elongated triangular bipyramid J14
JBTPR-8	9 C2v	Biaugmented trigonal prism J50
BTPR-8	10 C2v	Biaugmented trigonal prism
JSD-8	11 D2d	Snub diphenoid J84
TT-8	12 Td	Triakis tetrahedron

Structure [ML8]:	HBPY-8	15.011
	CU-8	8.872
	SAPR-8	1.340
	TDD-8	1.344
	JGBF-8	15.665
	JETBPY-8	26.840
	JBTPR-8	2.433
	BTPR-8	1.861
	JSD-8	4.121
	TT-8	9.619

Dy2:

HBPY-8	3 D6h	Hexagonal bipyramid
CU-8	4 Oh	Cube
SAPR-8	5 D4d	Square antiprism
TDD-8	6 D2d	Triangular dodecahedron
JGBF-8	7 D2d	Johnson gyrobifastigium J26
JETBPY-8	8 D3h	Johnson elongated triangular bipyramid J14
JBTPR-8	9 C2v	Biaugmented trigonal prism J50
BTPR-8	10 C2v	Biaugmented trigonal prism
JSD-8	11 D2d	Snub diphenoid J84
TT-8	12 Td	Triakis tetrahedron

Structure [ML8]:	HBPY-8	15.922
	CU-8	10.621
	SAPR-8	2.099
	TDD-8	1.067
	JGBF-8	14.168
	JETBPY-8	28.353
	JBTPR-8	2.058
	BTPR-8	1.617
	JSD-8	3.339
	TT-8	11.354

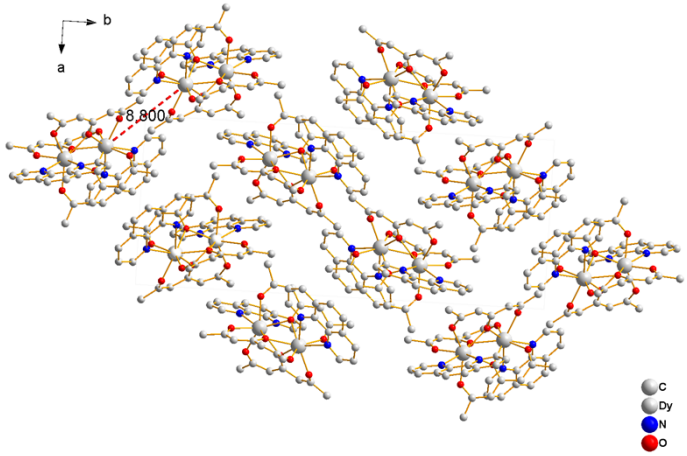

Fig. S1 Packing arrangement of complex **1** along the *c* axis, hydrogen and fluorine atoms are omitted for clarity, the dotted line is the shortest intermolecular Dy-Dy distance.

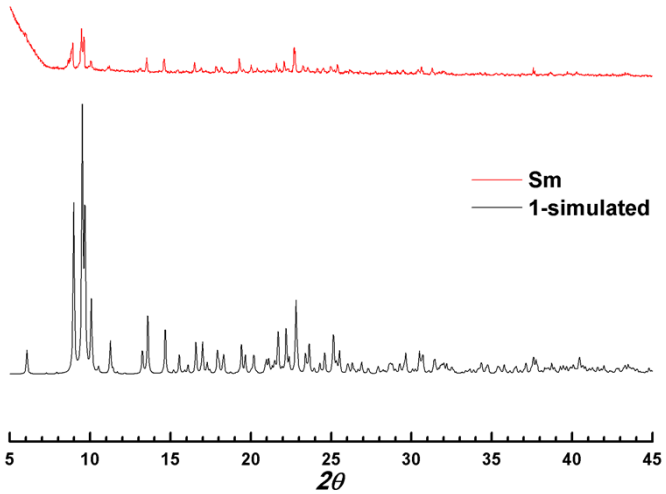

Fig. S2 Powder XRD analysis of **3**. The black line is simulated data from single crystal data of **1**.

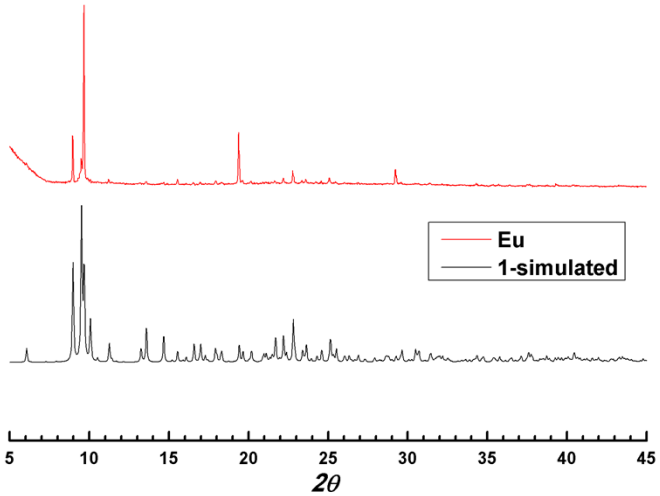

Fig. S3 Powder XRD analysis of **4**. The black line is simulated data from single crystal data of **1**.

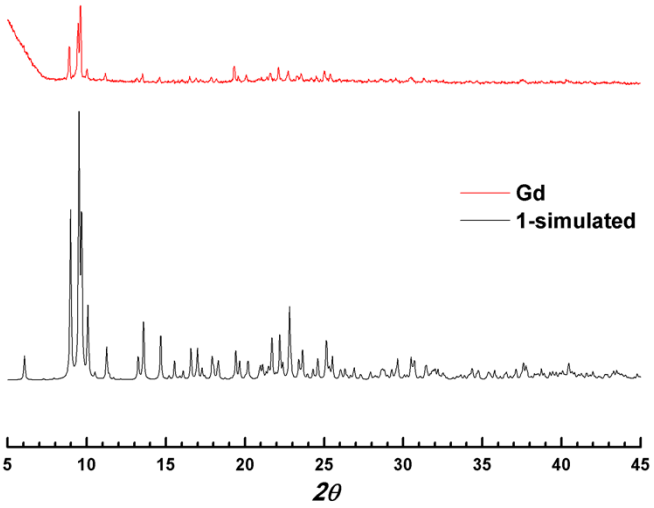

Fig. S4 Powder XRD analysis of **5**. The black line is simulated data from single crystal data of **1**.

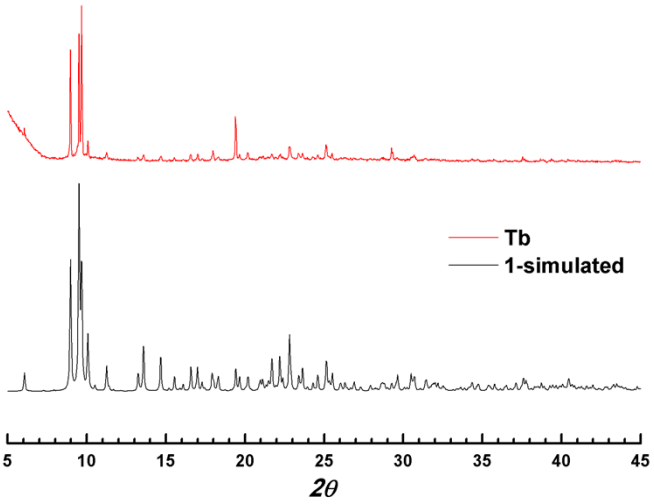

Fig. S5 Powder XRD analysis of **6**. The black line is simulated data from single crystal data of **1**.

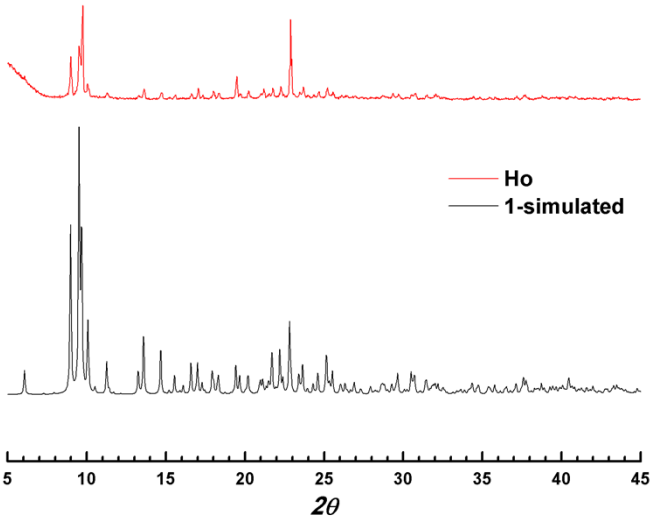

Fig. S6 Powder XRD analysis of **7**. The black line is simulated data from single crystal data of **1**.

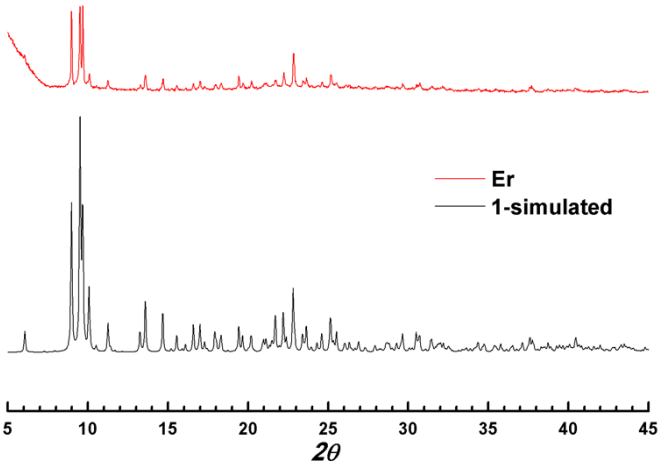

Fig. S7 Powder XRD analysis of **8**. The black line is simulated data from single crystal data of **1**.

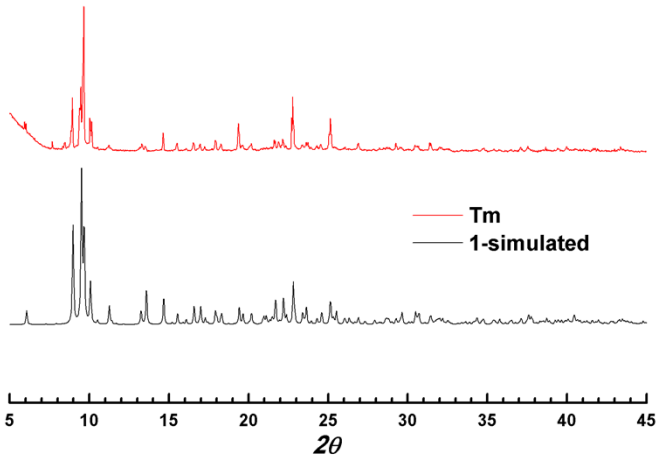

Fig. S8 Powder XRD analysis of **9**. The black line is simulated data from single crystal data of **1**.

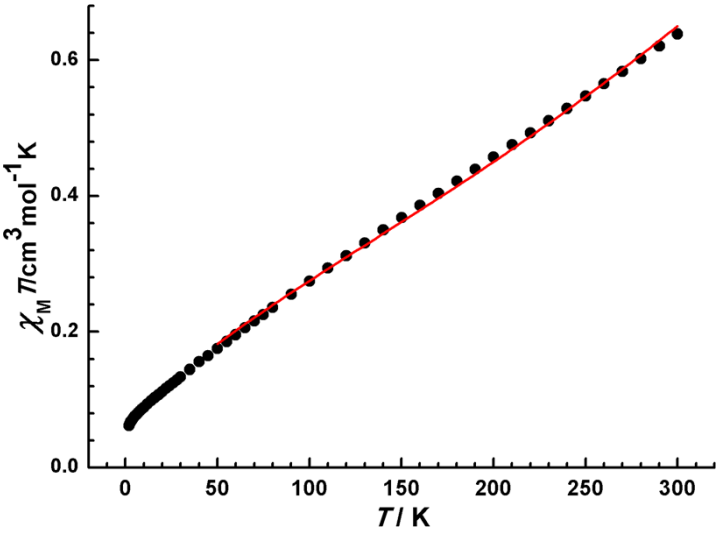

Fig. S9 $\chi_M T$ versus T curve of complex **3**, the red line is the best simulation in the temperature range 50-300 K with the parameters of λ = 224.3 cm^{-1}, g = 0.33, zj' = -2.68 cm^{-1}.

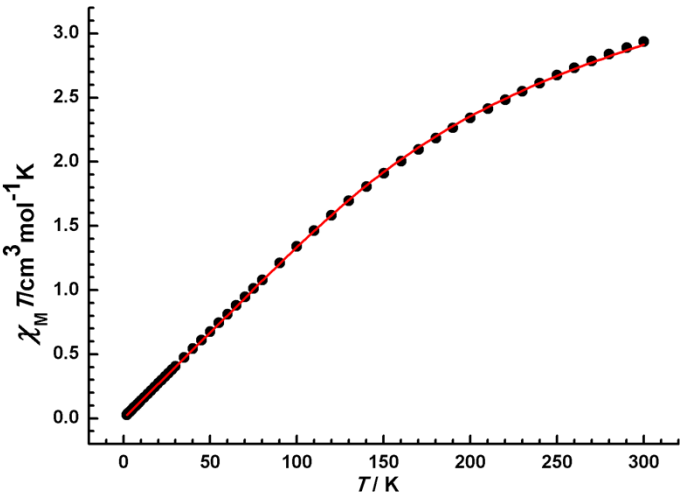

Fig. S10 $\chi_M T$ versus T curve of complex **4**, the red line is the best simulation in the temperature range 2-300 K with the parameters of λ = 346.9 cm^{-1}, g = 0.79, zj' = 1.38 cm^{-1}.

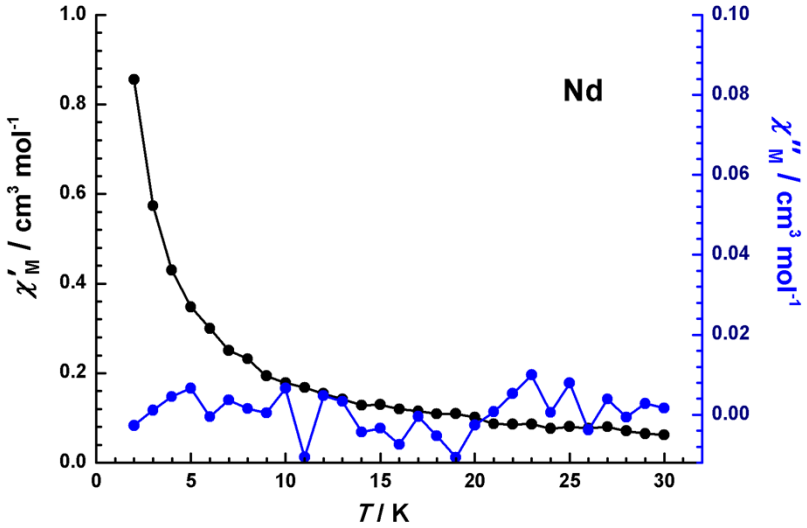

Fig. S11 Temperature dependence of the in-phase (χ') and out-of-phase (χ") components of the alternating-current susceptibilities for complex **2** under zero *dc* field at the frequency of 1000 Hz.

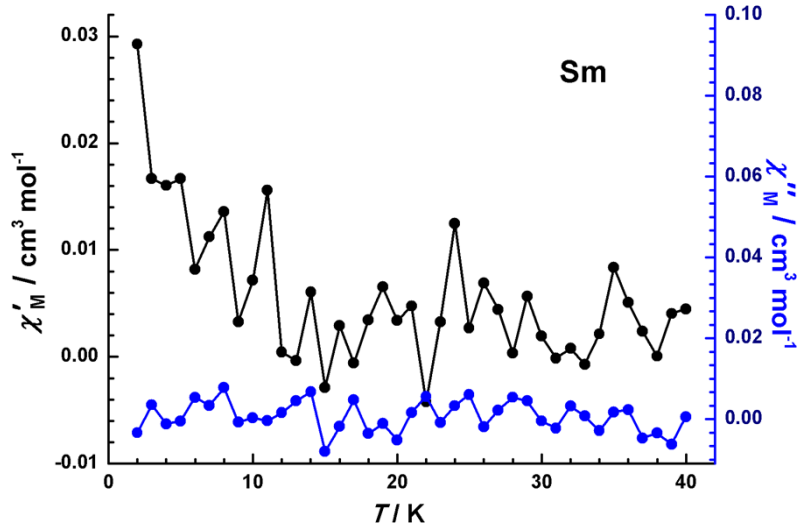

Fig. S12 Temperature dependence of the in-phase (χ') and out-of-phase (χ") components of the alternating-current susceptibilities for complex **3** under zero *dc* field at the frequency of 1000 Hz.

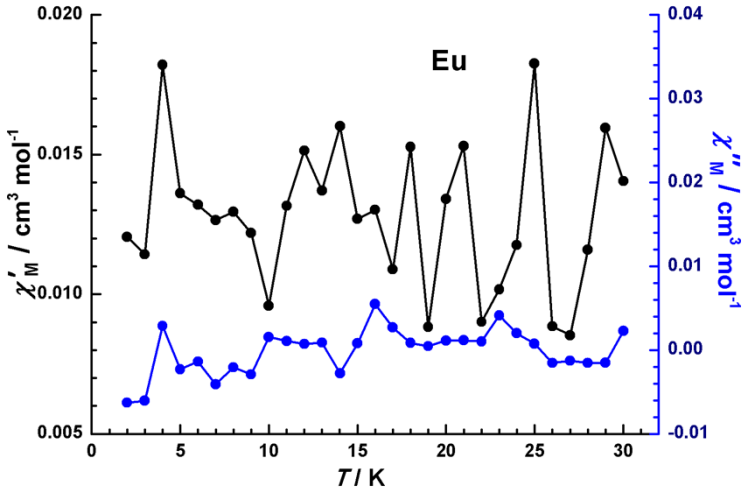

Fig. S13 Temperature dependence of the in-phase (χ') and out-of-phase (χ") components of the alternating-current susceptibilities for complex **4** under zero *dc* field at the frequency of 1000 Hz.

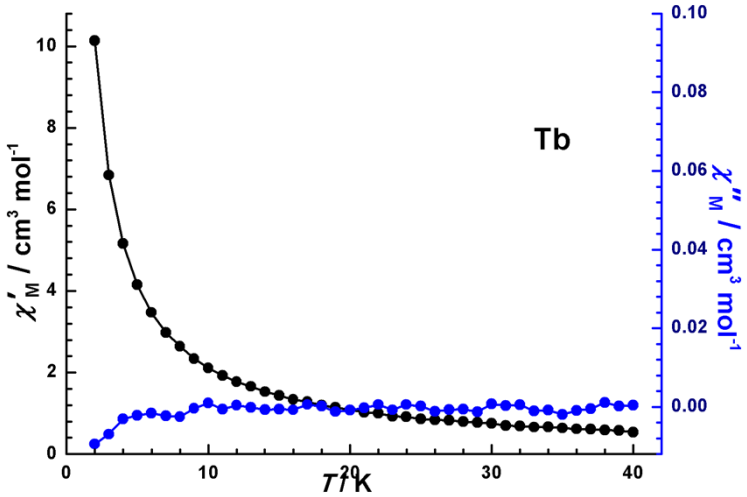

Fig. S14 Temperature dependence of the in-phase (χ') and out-of-phase (χ") components of the alternating-current susceptibilities for complex **6** under zero *dc* field at the frequency of 1000 Hz.

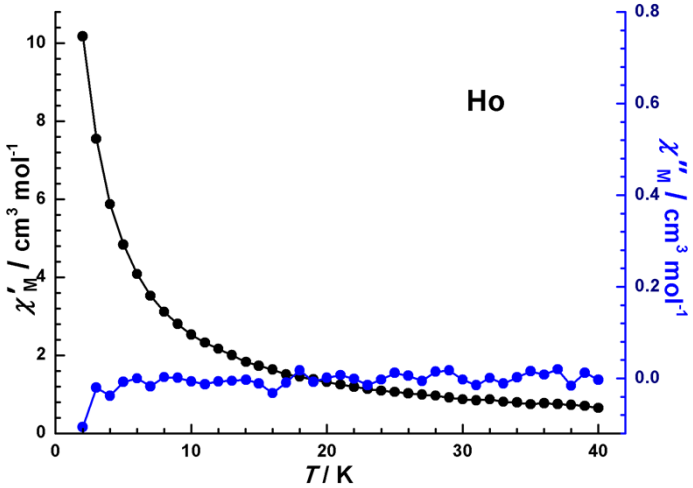

Fig. S15 Temperature dependence of the in-phase (χ') and out-of-phase (χ") components of the alternating-current susceptibilities for complex **7** under zero *dc* field at the frequency of 1000 Hz.

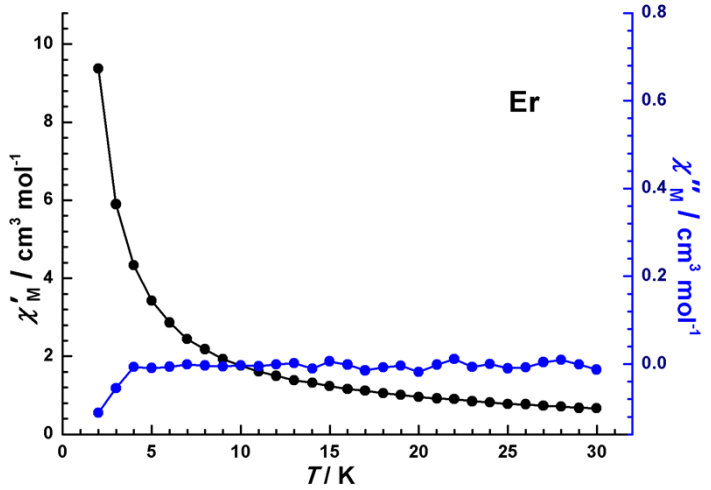

Fig. S16 Temperature dependence of the in-phase (χ') and out-of-phase (χ") components of the alternating-current susceptibilities for complex **8** under zero *dc* field at the frequency of 1000 Hz.

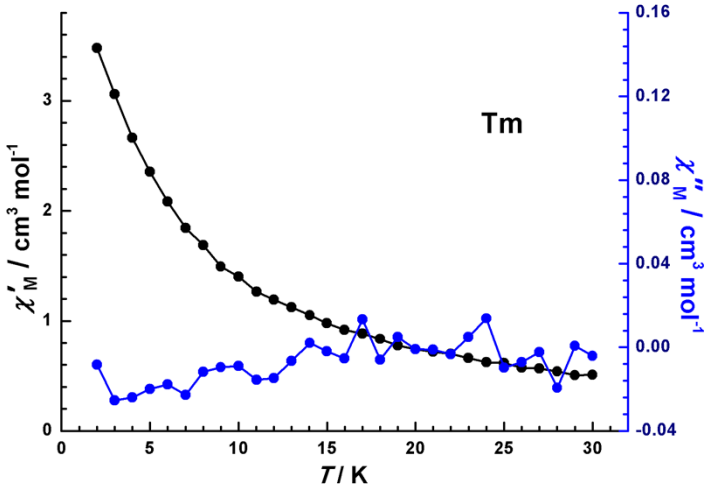

Fig. S17 Temperature dependence of the in-phase (χ') and out-of-phase (χ") components of the alternating-current susceptibilities for complex **9** under zero *dc* field at the frequency of 1000 Hz.

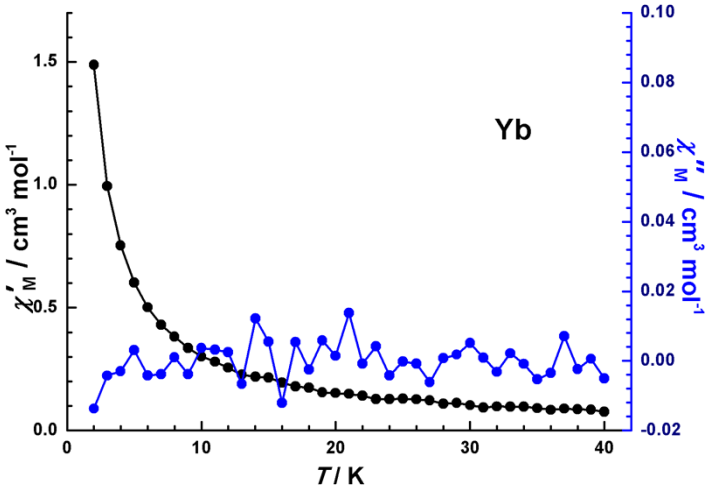

Fig. S18 Temperature dependence of the in-phase (χ') and out-of-phase (χ") components of the alternating-current susceptibilities for complex **10** under zero *dc* field at the frequency of 1000 Hz.